Supplementary Information

Reduced lattice thermal conductivity and strong four-phonon scattering in *h*-B_{12} assembled by boron clusters on a honeycomb lattice

Ting Zhang [a], *Yu-Run Yang* [a], *Xu Liu* [a], *Jing Wang* [*a], *Zhao Liu* [*ab], *and Ying Liu* [ac]

[a] Department of Physics and Hebei Advanced Thin Film Laboratory, Hebei Normal University, Shijiazhuang, 050024, China

[b] Beijing Computational Science Research Center, Beijing, 100193, China

[c] National Key Laboratory for Materials Simulation and Design, Beijing, 100083, China

* Corresponding author: zliu@hebtu.edu.cn and jwang@hebtu.edu.cn

SI. Convergence calculations of κ_{lat} about q-points.

We can see that the κ_{lat} of 2D *h*-B_{12} is converged to within 5% for an increase in **q**-points beyond $90 \times 90 \times 1$ when considering only 3ph scattering. Additionally, it is converged to within 5% for an increase in **q**-points beyond $22 \times 22 \times 1$ when considering both 3ph and 4ph scatterings.

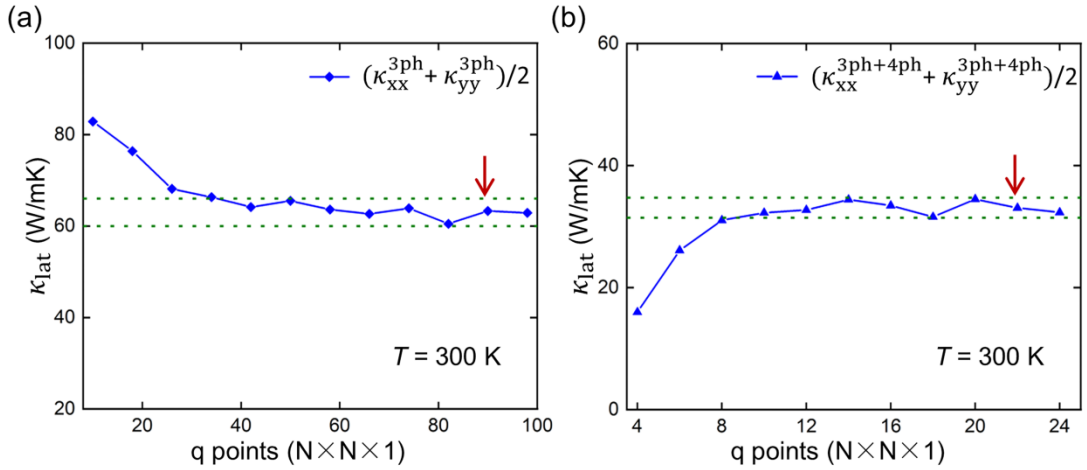

Fig. S1 Variation of κ_{lat} with different **q**-points for 2D *h*-B_{12}, considering (a) only 3ph scattering and (b) both 3ph and 4ph scattering processes. The red arrow indicates the selected **q**-points, and the green dashed line represents a fluctuation of ±5% around the converged value.

S2. Basic information on the three structures assembled from icosahedral B_{12} clusters.

Figure S2(a) displays the optimized 2D honeycomb structure of *h*-B_{12}, the triangular structure of *t*-B_{12}, and the kagome structure of *k*-B_{12} from left to right. All three structures are assembled from the icosahedral B_{12} clusters as the basic building unit. Table S1 lists the space group, lattice constants, atomic layer thickness, and the B-B bonding lengths for adjacent clusters after comprehensive optimization for *h*-B_{12}, *t*-B_{12}, and *k*-B_{12}. Figure S2(b) shows the phonon dispersions of the three structures in Fig. S2(a), We found that only *h*-B_{12} has no imaginary frequencies, proving its stability. Figure S2(c) displays the band structures of three structures in Fig. S2(a) calculated using the PBE0 functional, revealing that the honeycomb *h*-B_{12} is an indirect bandgap semiconductor ($\Delta = 1.07$ eV), while the triangular *t*-B_{12} and kagome *k*-B_{12} are metallic. Therefore, the main carriers of thermal transport in *h*-B_{12} are phonons. Notably, at the K point, there are two Dirac states labeled as D_1 (1.7 eV above the Fermi level) and D_2 (1.4 eV below the Fermi level). Furthermore, the group velocities at D_1 (2.75×10^5 m/s) and D_2 (1.31×10^5 m/s) are only one order of magnitude lower than the Fermi velocity in graphene,[1] suggesting that *h*-B_{12} is likely to exhibit high electrical conductivity. Additionally, *h*-B_{12} exhibits a stronger spin-orbit coupling (SOC) effect compared to graphene and silicon, with a Rashba coefficient of approximately 1.8 eV/Å, which is greater than or at least comparable to that of many well-known strong SOC materials.[2-6] The aforementioned results can also be found in Fig. 2 of Ref. 32 in the manuscript. This work presents the thermal

transport properties of *h*-B_{12}, using first-principles calculations in conjunction with the Boltzmann Transport Equation (BTE) method.

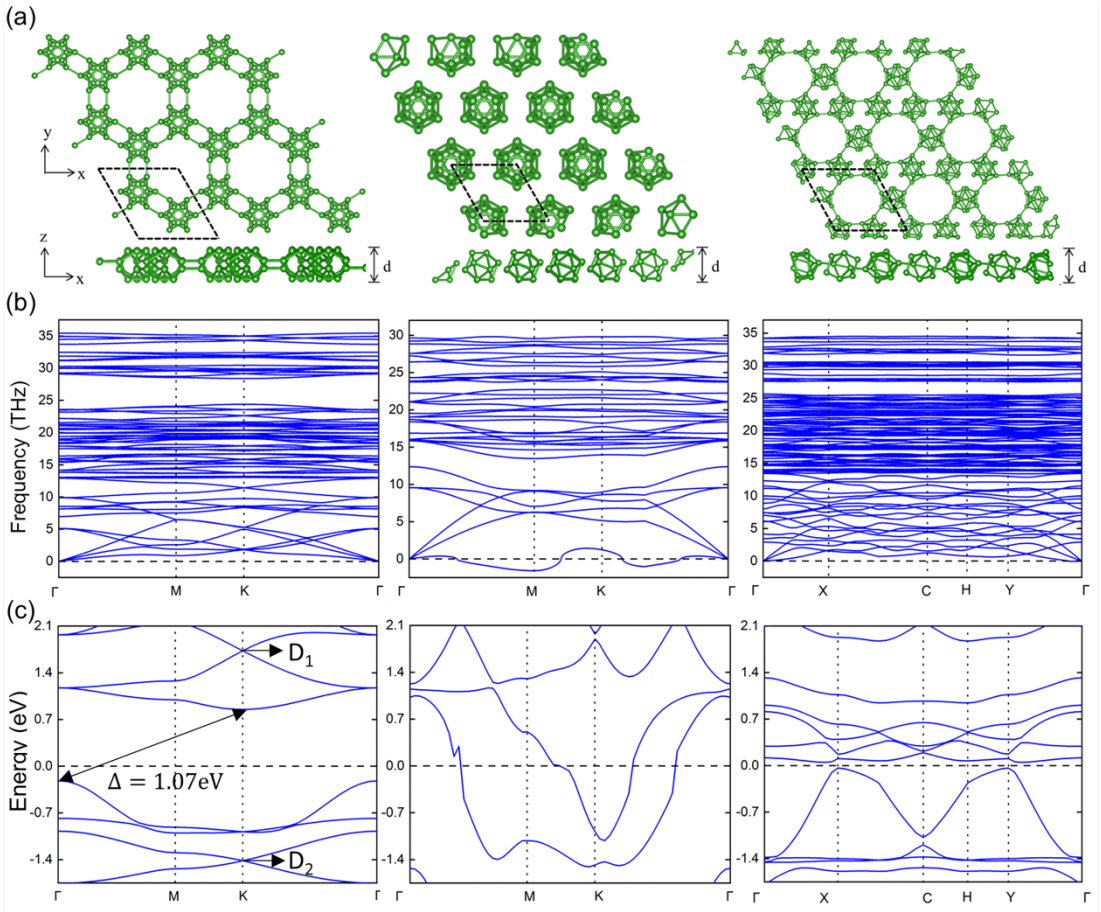

Fig. S2 (a) Top and side views of 2D *h*-B_{12} (left), *t*-B_{12} (middle), and *k*-B_{12} (right), with *d* representing the atomic layer thickness, the black rhombic dashed box indicates the unit cell. (b) Phonon dispersions of 2D *h*-B_{12} (left), *t*-B_{12} (middle), and *k*-B_{12} (right). (c) Band structures of 2D *h*-B_{12} (left), *t*-B_{12} (middle), and *k*-B_{12} (right), referenced to the Fermi energy. In the band structure of *h*-B_{12}, two Dirac states are marked as D_1 (1.7 eV above the Fermi level) and D_2 (1.4 eV below the Fermi level).

Table S1. The parameters of the three structures in Fig. S2(a).

Structure	**Space group**	***a* (Å)** [a)]	***b* (Å)** [a)]	***d* (Å)** [a)]	**B-B (Å)** [a)]
h-B_{12}	$P\bar{3}1m$	8.28	8.28	2.45	1.71
t-B_{12}	$P\bar{3}m1$	4.78	4.78	2.46	1.93
k-B_{12}	*C2/m*	9.49	9.20	3.00	1.69

[a)] "***a***" and "***b***" represent the lattice constants, "***d***" is the thickness of the atomic layer, and "B-B" refers to the bond length of B-B bonds connecting adjacent clusters.

S3. Three types of bonds in *h*-B_{12}.

The unit cell of *h*-B_{12} contains two mirror-symmetric B_{12} clusters. Each B_{12} cluster in this structure is connected to three adjacent B_{12} clusters through two B–B bonds, with a bond length of 1.71 Å, which is in the range of B-B σ bonds. Within each B_{12} cluster, six weak covalent bonds persist in the *xy* plane, with an average B-B bond length of 1.90 Å. Notably, the top/bottom-most B-triangle features a bond length of 1.60 Å.

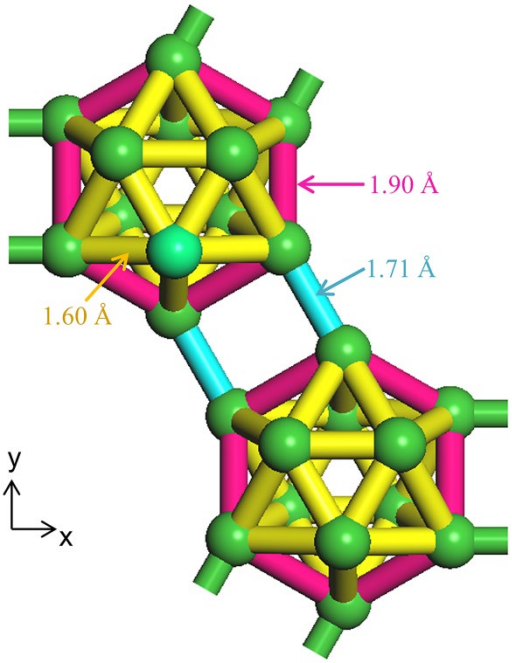

Fig. S3 Blue represents the bonds connecting each B_{12} cluster; pink indicates the six weak covalent bonds within the *xy* plane inside the B_{12} cluster; and yellow denotes the B-B bonds formed by the top/bottom B triangles within the B_{12} cluster.

References

[1] J. R. F. Lima, Phys. Lett. A 2015, **379**, 1372.

[2] Q. Liu, Y. Guo, and A. J. Freeman, Nano Lett. 2013, **13**, 5264.

[3] S. Singh and A. H. Romero, Phys. Rev. B 2017, **95**, 165444.

[4] F.-X. Xiang, X.-L. Wang, M. Veldhorst, S.-X. Dou, and M. S. Fuhrer, Phys. Rev. B 2015, **92**, 035123.

[5] L. G. D. da Silveira, P. Barone, and S. Picozzi, Phys. Rev. B 2016, **93**, 245159.

[6] A. Narayan, Phys. Rev. B 2015, **92**, 220101.